Traversing the Red–Green–Blue Color Spectrum in Rationally Designed Cupredoxins

Karl Koebke, Victor Sosa Alfaro, Tyler Pinter, Aniruddha Deb, Nicolai Lehnert, Cédric Tard, James Penner-Hahn, Vincent Pecoraro

Traversing the Red–Green–Blue Color Spectrum in Rationally Designed Cupredoxins

Karl J. Koebke,[a] Victor Sosa Alfaro,[a] Tyler B. J. Pinter,[a] Aniruddha Deb,[a] Nicolai Lehnert,[a] Cédric Tard,[b] James E. Penner-Hahn,[a] and Vincent L. Pecoraro*[a]

a: Department of Chemistry, University of Michigan Ann Arbor, MI 48109
b: LCM, CNRS, Ecole Polytechnique, IP Paris, F-91128 Palaiseau, France
* corresponding author: vlpec@umich.edu

Abstract

Blue copper proteins have a constrained Cu(II) geometry that has proven difficult to recapitulate outside native cupredoxin folds. Previous work has successfully designed green copper proteins which could be tuned blue using exogenous ligands, but the question of how one can create a self-contained blue copper site within a de novo scaffold, especially one removed from a cupredoxin fold, remained. We have recently reported a red copper protein site within a three helical bundle scaffold which we later revisited and determined to be a nitrosocyanin mimic, with a $CuHis_2CysGlu$ binding site. We now report efforts to rationally design this construct toward either green or blue copper chromophores using mutation strategies that have proven successful in native cupredoxins. By rotating the metal binding site, we created a de novo green copper protein. This in turn was converted to a blue copper protein by *removing* an axial methionine. Following this rational sequence, we have successfully created red, green, and blue copper proteins within an alpha helical fold, enabling comparisons for the first time of their structure and function disconnected from the overall cupredoxin fold.

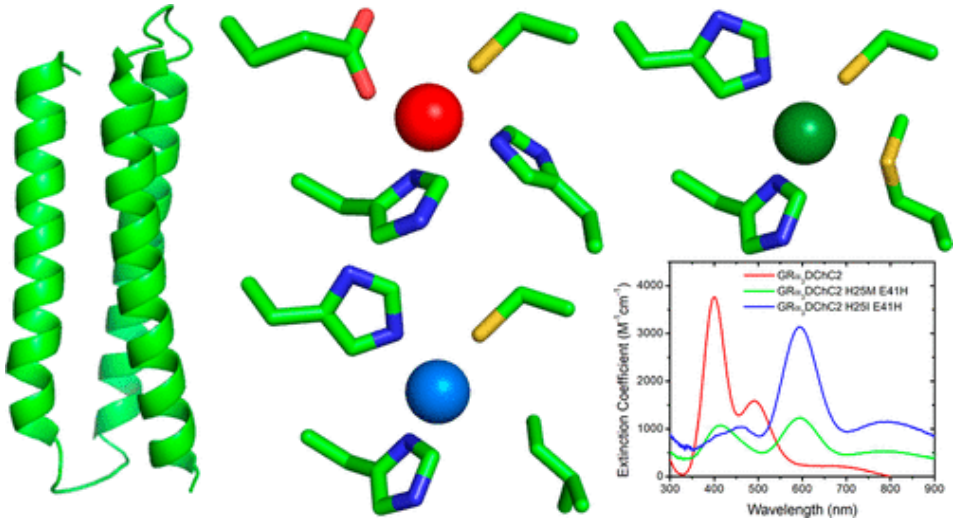

Introduction

Cupredoxins are copper binding electron transfer proteins found in bacteria, archaea, algae, plants, and animals. They are involved in essential life processes, such as the nitrogen cycle, photosynthesis, and respiration.[1,2] These metalloproteins have long fascinated the bioinorganic community due to their constrained metal binding centers and uniquely intense optical absorption bands leading to deep blue, green, or red colors.[3,4] All cupredoxins have a His_2CysX_n Cu metal binding site in common, but the color of the bound Cu(II) depends on the energy and relative intensity of LMCT bands caused by interactions between the $d_{x^2-y^2}$ orbital of Cu and the σ or π molecular orbitals of the bound deprotonated Cys. This spectroscopic difference is linked to the strength of the Cu–Cys bond, as illustrated by the following series of native examples.

Poplar plastocyanin is a blue copper protein with a $CuHis_2CysMet$ binding site, a low intensity absorption band at 460 nm and a high intensity band at 597 nm, with an intensity ratio ($\varepsilon_{\sigma/\pi}$) between these transitions of 0.05, and an exceptionally short Cu(II)–Cys distance of 2.08 Å.[5,6] Stellacyanin is an example of a perturbed blue copper protein with a $CuHis_2CysGln$ binding site, absorption bands at 448 and 604 nm with a $\varepsilon_{\sigma/\pi}$ of 0.29, and a slightly longer Cu(II)–Cys distance of 2.17 Å.[7,8] The electron transfer center within Cu nitrite reductase is a green copper with a $CuHis_2CysMet$ binding site, absorption bands of roughly equal intensity at 457 and 570 nm with a $\varepsilon_{\sigma/\pi}$ of 1.74, and a Cu(II)–Cys distance of 2.22 Å.[9,10] Comparisons of blue to green cupredoxins have led to the "coupled distortion" model in which the strength of the axial ligand is inversely correlated to the strength of the Cu(II)–Cys bond which correlates to the observed absorption spectra.[3] All blue to green cupredoxins are also characterized by compressed ($<100 \times 10^{-4}$ cm^{-1}) hyperfine coupling constants in EPR linked to their relatively covalent Cu(II)–Cys bonds, apparent reduction potentials in a relatively large range from +184 to +580 mV, and binding sites where His_2Cys take equatorial positions with a variable residue in the axial position.[3,11,12] Nitrosocyanin is possibly the most distinct of the native monatomic cupredoxins with a red copper center comprised of HisGluCys equatorial residues and a His in the axial position (a rotation of the His_2Cys binding trimer seen in blue and green cupredoxins depicted in Figure 1), an intense absorption band at 390 nm and a smaller band at 490 nm with a $\varepsilon_{\sigma/\pi}$ of 3.18, an uncompressed hyperfine coupling constant at 142×10^{-4} cm^{-1}, and a longer Cu(II)–Cys bond of 2.30 Å.[13,14] Lastly, there are purple cupredoxins which typically have a binuclear copper site and more recently a mononuclear variant with an open binding site was discovered within the nitrifying archaeon *Nitrosopumilus maritimus*, but these were not included in the design efforts in this manuscript.[15–19]

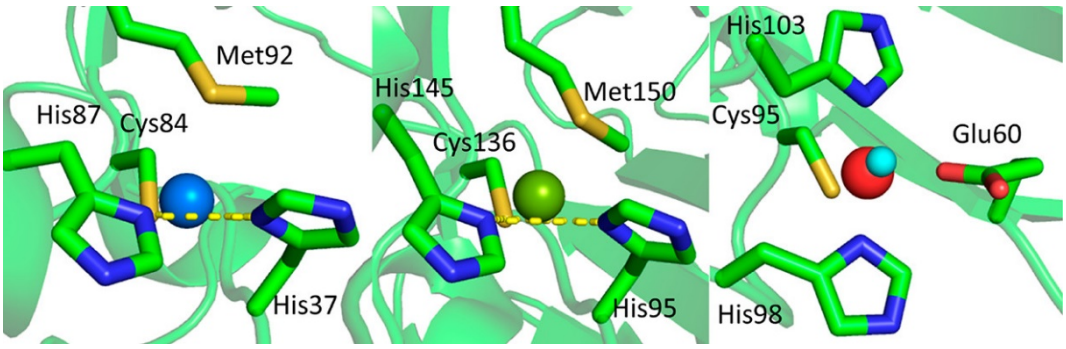

Figure 1. Pymol illustrations of the Cu binding sites of (A) plastocyanin (pdb 4dpb), (B) Cu nitrite reductase (pdb 1sjm), and (C) nitrosocyanin (pdb 1iby). Cu(II) ions are depicted as blue, green, or red spheres, water as a cyan sphere, and the $N_\delta His–N_\delta His–Cys$ plane is illustrated as a dashed line to emphasize the difference in Cu(II) positioning in plastocyanin and Cu nitrite reductase.

Mutation studies of native cupredoxins have determined that controlling the nature of the Cu–Cys interaction, which defines their character, is accomplished through the relative orientation of the metal binding site, and the identity and strength of the fourth coordinating ligand.[3] These three cupredoxin groupings (blue, green, and red) can be interconverted via changes in axial residues; green cupredoxins can be converted to blue by decreasing the coordinating strength of the axial ligand (such as M182T Cu nitrite reductase[20,21]), or blue sites can be turned to red by increasing the axial ligand bond (such as M148E rusticyanin and M121E azurin[12,22]). A more drastic rearrangement of the binding site of azurin was recently described by the Lu laboratory. They demonstrate the conversion of a blue cupredoxin to the spectroscopic properties and geometry of nitrosocyanin (red), which allowed them to make inferences on the NO binding properties of the native protein.[23] In every one of these derivatives a native cupredoxin fold was modified to convert between sites of different physical properties. To date, there are no examples of "blue" copper sites in folds differing from the β-sheet structures associated with the native proteins without the addition of exogenous ligands.

Another strategy by which one can investigate the core question of the relationship between structure and function in proteins is by de novo design. De novo metalloprotein design is a means of studying the metal binding site within a protein environment unrelated to the native fold.[24] Given the well-studied nature of cupredoxins, and how the varying types differ in geometry, we should be able to design any variant of cupredoxin within an unrelated, or de novo, fold. Several laboratories have attempted to design a blue copper protein within a de novo fold, but almost all culminate in green copper proteins ($\varepsilon_{\sigma/\pi} \approx 1$).[25–27] Recent work from Shiga and Tanaka showed that one could create a green copper protein within a four-α-helical-bundle, but also that through the addition of exogenous ligands such as Cl^- one could tune the spectroscopic properties of this construct to that of a blue copper protein ($\varepsilon_{\sigma/\pi} \leq 0.4$).[28,29]

Recently, we designed a red copper protein using the de novo scaffold α_3DChC2.[30] Through mutation studies of a more stable GRα_3DChC2 derivative, we determined that the red copper-like spectrum of α_3DChC2 was due to a His_2CysGlu copper binding site, with an unexpected interaction from a surface Glu41.[31] This Cu(II)-Glu41 interaction was necessary to maintain the red copper-like Cu(II) spectrum within our construct, and variants with E41A or E41Q mutations exhibited Type 2 Cu spectra. These results, as well as the MCD analysis of our construct, led to the conclusion that we had recapitulated the binding site of nitrosocyanin as opposed to a blue copper protein variant such as M148E rusticyanin or M121E azurin, which would have led to blue constructs when the strength of the Glu41 ligand was decreased through E41A or E41Q mutations.[12,22] In this work, we utilize this understanding of GRα_3DChC2 as a nitrosocyanin mimic to explore methods by which a de novo red copper protein can be converted into a green or blue copper protein. In doing so, we have created a green copper protein within GRα_3D which we tune further to create the first de novo blue copper protein that does not require an exogenous ligand. The ability to transplant red, green, or blue copper protein sites by design into the same de novo scaffold is a major advance in metalloprotein design, one which opens up a plethora of possible comparisons and studies of these sites in protein environments, divorced from their native secondary or tertiary structures.

Materials and Methods

All reagents were purchased from Sigma-Aldrich or Fisher Scientific unless otherwise specified.

Molecular Biology/Purification

Genes used in this study were introduced to an existing plasmid by reverse PCR before using the In-Fusion (ClonTech) protocol to recyclize the resulting mutated plasmid. Mutated plasmids were transformed into BL21 (DE3) *Escherichia coli* and then sequenced by Sanger Sequencing at the University of Michigan DNA Sequencing Core. Constructs were expressed and purified using previously published methods.[31,32]

Spectroscopy

Electronic absorption data were collected with a Cary 100 UV–visible absorption spectrometer on solutions containing 75 μM peptide, 50 μM Cu(II) acetate, and 50 mM buffer (HEPES at pH 7.5, MES at pH 5.5 or 6.5, or CHES at pH 9.0 or 10.0). Circular Dichroism (CD) measurements were taken using a Jasco J-1500 CD Spectropolarimeter on solutions containing 10 μM peptide and 10 mM buffer (potassium phosphate at pH 5.5 or 7.5 or boric acid at pH 10). Electron paramagnetic resonance spectra were collected using a Bruker EMXE 200 EPR spectrometer, on solutions containing 500 or 750 μM Cu(II)Acetate, 750 μM or 1 mM peptide, 30% glycerol, and 50 mM buffer (HEPES at pH 7.5, MES at pH 5.5 or 6.5, or CHES at pH 9.0 or 10.0). The EPR spectra were processed using the software SpinCount (Prof. Michael Hendrich, Carnegie Mellon University). The simulations were also performed using

SpinCount to determine the $g_{\|}$, $g_{\perp}$, $A_{\|}$, and $A_{\perp}$ values. Mass and purity of peptide solutions were determined by Micromass LCT TOF MS.

X-ray Absorption Spectroscopy

Cu(I) samples were prepared with a final concentration of 1 mM Tetrakis(acetonitrile)Cu(I) hexafluorophosphate, 1.5 mM peptide solution in 50 mM HEPES buffer at pH 7.5 with 50% glycerol (added as a glassing agent) in an anaerobic glovebox. Sample solutions were loaded into a sample cell and frozen in liquid nitrogen. These solutions included 0.5 mM excess apo peptide to ensure free Cu(I) concentration was minimal (<0.01%).

Cu(II) samples were prepared with final concentrations of 1 mM Cu(II)acetate and 1.5 mM peptide in 50 mM HEPES buffer at pH 7.5 in aerobic conditions. Samples were lyophilized before transferring to sample cells. During collection the Cu edge energy and 1s → 4p transition of Cu(I) peptide were monitored. We estimate that less than 10% of the sample was photoreduced by the final scan included in fitting.

Measurements were carried out at Stanford Synchrotron Radiation Lightsource (SSRL) beamline 9–3 with a Si(220) double-crystal monochromator and a flat Rh-coated harmonic rejection mirror. Samples were maintained below 10 K with an Oxford Instruments liquid helium cryostat. Data were measured as fluorescence excitation spectra using a 100-element Ge detector array normalized to incident intensity measured with a N_2 filled ion chamber. Data were measured with steps of 0.25 eV in the XANES region (1 s integration time) and 0.05 $Å^{-1}$ in the EXAFS region to k = 13.5 $Å^{-1}$ (1–20 s integration, k^3 weighted). Energies were calibrated by assigning the lowest energy inflection point of a copper metal foil as 8980.3 eV. The threshold energy, E_0, was defined as 8991 based on fits of model compounds; this was used to convert data to k-space, and the background was removed using a 3-region cubic spline. EXAFS data were analyzed using EXAFSPAK[33] and FEFF 9.0.[34] XANES data were normalized using MBACK.[35]

Single- and multiple-scattering fitting of EXAFS data were performed using EXAFSPAK[33] with ab initio amplitude and phase parameters calculated using FEFF 9.0.[34] An initial model of Cu–imidazole coordination was built based on the averaged bond distances determined by single-scattering fitting of EXAFS data.

Electrochemical Experiments

Cyclic voltammograms were measured on an AUTOLAB PGSTAT 30 (Metrohm, Herisau, Switzerland) using protein-film voltammetry techniques. The electrochemical setup consisted of a gold disc working electrode (0.00196 cm^2), a platinum wire counter electrode, and an aqueous saturated calomel electrode (SCE) as the reference electrode (0.241 V + SCE = normal hydrogen electrode) in an argon-saturated buffer (100 mM HEPES pH 7.5, 100 mM Na_2SO_4) measured under argon atmosphere. The gold electrode surface was polished using three successively finer polishing cloths and diamond-slurries, and sonicated in ethanol. To ensure surface homogeneity, the polished electrodes were scanned in 500 mM H_2SO_4 from −300 to +1500 mV (vs SCE) at 200 mV/s, until successive scans overlaid, and then in a cell which contained 0.1 M phosphate buffer (pH 7.4) and 0.1 M Na_2SO_4 by scanning four times from −300 to +600 mV (vs SCE) at 100 mV/s. Peptide stock solutions were prepared fresh daily in argon saturated buffer. Ten µL of copper protein solution (500 µM peptide, 450 µM Cu(II), 2 mM ascorbate, 100 mM HEPES pH 7.5) was incubated onto dried homogeneous gold electrodes under argon atmosphere and allowed to incubate for 2 h before being carefully rinsed with DI H_2O. Cyclic voltammograms were collected at various scan rates from 0.02 to 1 V/s at room temperature (22 °C).

Results

Cu(II) Spectroscopy and Electrochemistry

Electronic absorption spectra were collected for Cu(II) bound versions of GRα$_3$DChC3, GRα$_3$DChC4, and GRα$_3$DChC5 (Figures 2, 3, and 4). The optical obsoption spectrum of the Cu(II)GRα$_3$DChC2 parent construct shows an intense band at 400 nm and a weaker absorbance at 490 nm. In comparison, Cu(II)GRα$_3$DChC3 has a blue-shifted absorption feature at 395 nm of similar intensity and a small band at 600 nm, increasing the intensity ratio of these bands to 3.80. Cu(II)GRα$_3$DChC4, however, exhibits an absorption feature at 410 nm of decreased intensity and a lower energy band at 594 nm of similar intensity, similar to the spectral properties of green cupredoxins from CuNiR. Adding 1 M NaCl to a solution of Cu(II)GRα$_3$DChC4 redshifts the higher energy band to 473 nm and increases the intensity of the lower energy band. This decreases the intensity ratio between the LMCT bands to 0.46. Cu(II)GRα$_3$DChC5 as well as its R24M and R24Y variants have a blue-shifted absorption feature at ~460 nm of low intensity and a higher intensity band at 595 nm reminiscent of the absorption profile of stellacyanin, sometimes categorized as a perturbed blue cupredoxin (Figure 4). Electronic absorption spectra of Cu(II) GRα$_3$DCh4 and GRα$_3$DChC5 R24Y were obtained at pH 5.5, 6.5, 7.5, 9.0, and 10.0 to determine the pH dependence of the multiple species indicated by EPR (vide infra). Decreasing the pH to 5.5 results in a decrease in intensity of the LMCT bands at both 460 and 595 nm, while increasing the pH to 10.0 results in a loss of the bands at 460 and 595 nm, paired with an increased intensity in a new band at 390 nm. Increasing NaCl concentration at pH 7.5 results in an increase in the LMCT band at 460 nm while the 595 nm band remains static.

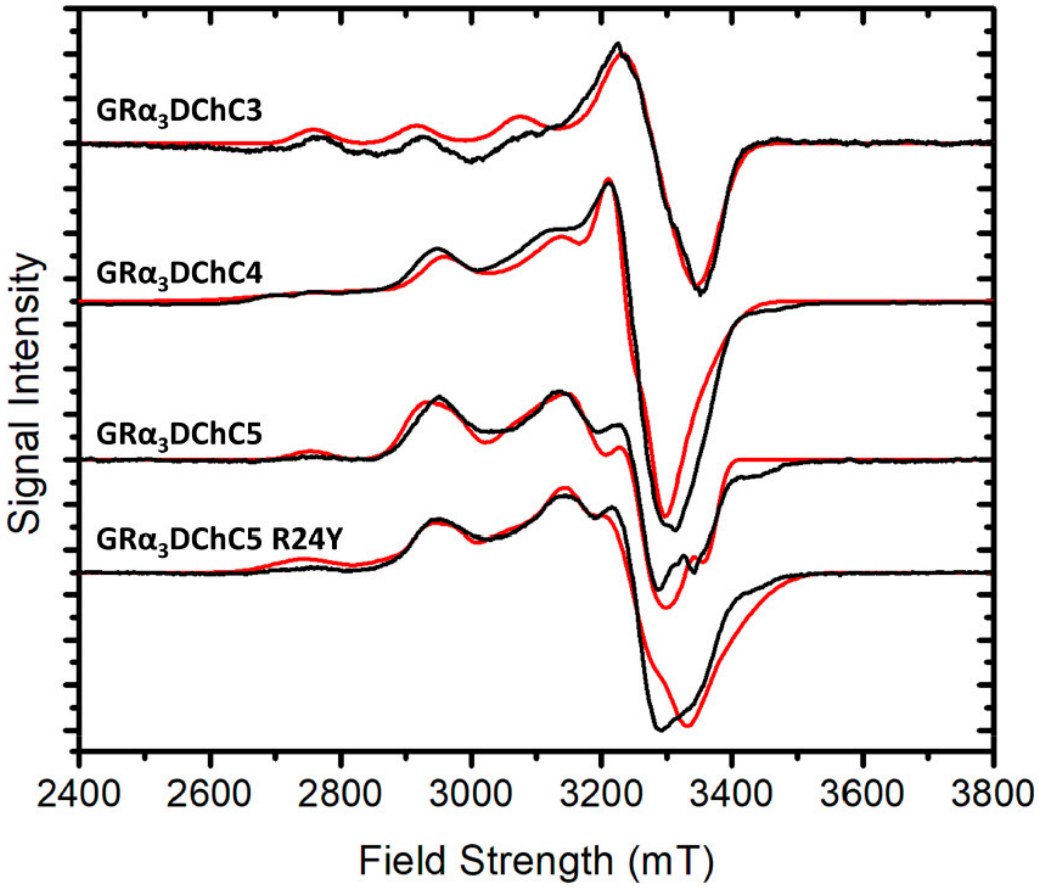

Figure 2. EPR spectra for all constructs reported within this manuscript with data in black and total simulated spectra in red. Solutions contained 750 µM Cu(II) and 1 mM peptide. EPR spectra were recorded using CW X-band collected at 9.30 MHz, 100 K, and 20.51 mW microwave power.

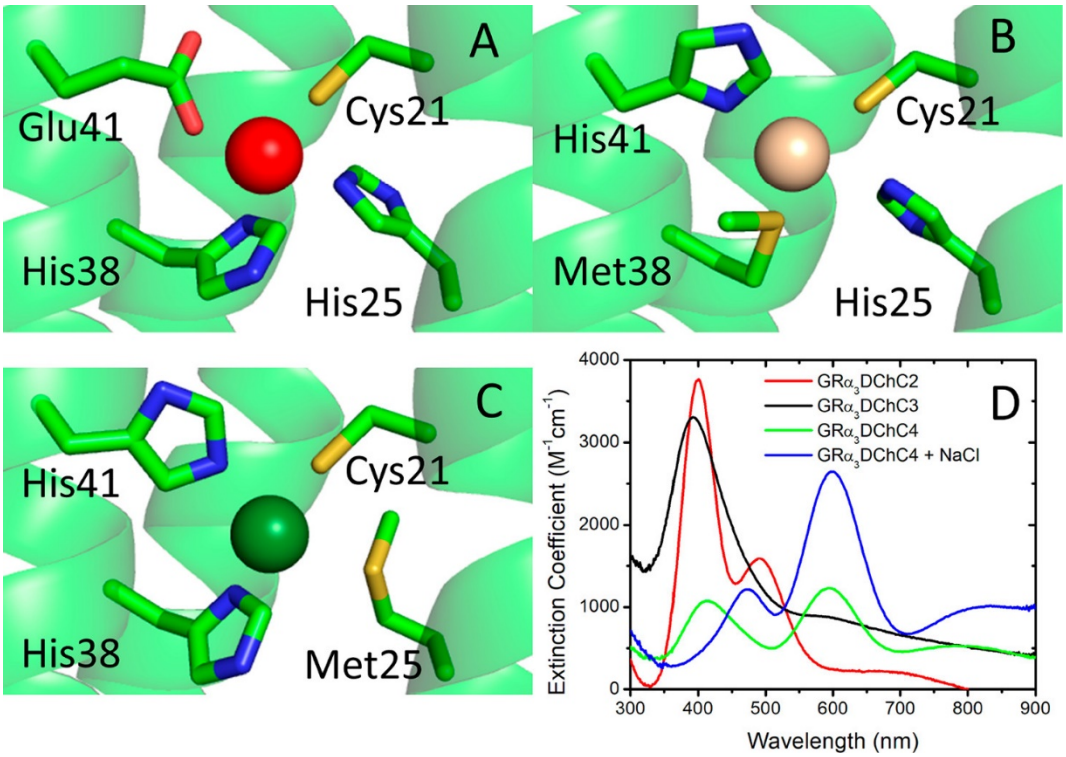

Figure 3. Pymol illustrations of the proposed Cu(II) binding sites of (A) GRα$_3$DChC2, (B) GRα$_3$DChC3, and (C) GRα$_3$DChC4 as well as a comparison of their optical absorption spectra (D). Pymol illustrations were created using the crystal structure of GRα$_3$D (PDB 6ds9).

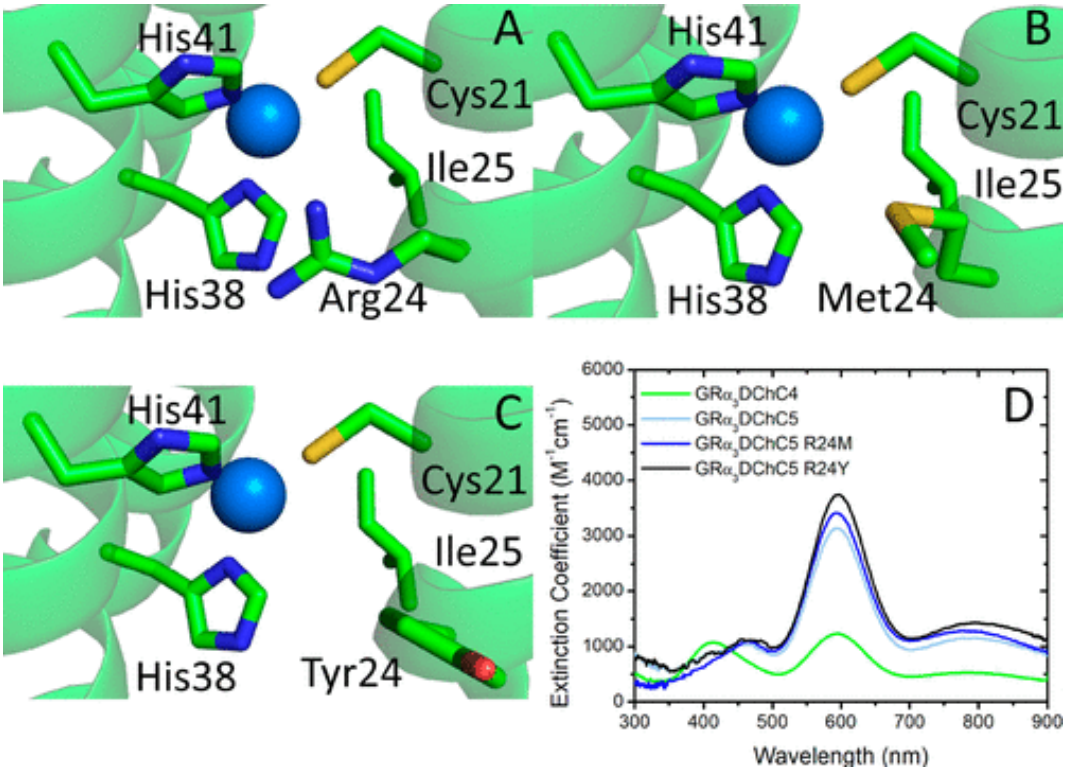

Figure 4. Pymol illustrations of the Cu(II) binding sites of (A) GRα$_3$DChC5, (B) GRα$_3$DChC5 R24M, and (C) GRα$_3$DChC5 R24Y as well as a comparison of their optical absorption spectra to that of GRα$_3$DChC4 (D). Pymol illustrations were created using the crystal structure of GRα$_3$D (pdb 6ds9).

Apparent standard potentials (E^0) for the Cu(II/I) couples of GRα$_3$DChC4 and GRα$_3$DChC5 grafted on a gold electrode were measured at pH 7.5 using protein film voltammetry and are listed in Table 1. The Au-grafted peptide formed a stable electroactive film as assessed by the proportionality of the peak current versus the scan rate (Figure S8). Constructs GRα$_3$DChC4 and GRα$_3$DChC5 showed similar E^0 values around 475 mV vs NHE, 55 mV lower than the GRα$_3$DChC2 construct. Large wave and cathodic to anodic peak separations (ΔE_p) ranging from 130 to 220 mV suggest sluggish electron transfers and non-Nernstian behavior, similar to our previous observations (Figure S8).[30] Similar to previous results for Cu proteins within three helical bundle and three-stranded coiled coil peptides from our laboratory, the reduction potentials all center around +500 mV vs NHE.

Table 1. Absorption and Electrochemical Parameters for Constructs reported compared to native proteins and GRα$_3$DChC2

construct	λ_{max} (ε)	λ_{max} (ε)	$\varepsilon_{\sigma/\pi}$	half-life of Cu(II) signal	E^0 (mV vs NHE)
GRα$_3$DChC2[31]	400 nm (3760)	490 nm (1600)	2.33	8 h	+530
GRα$_3$DChC3	395 nm (3300)	600 nm (870)	3.80	5 min	
GRα$_3$DChC4	410 nm (1070)	595 nm (1230)	0.87	15 min	+475
GRα$_3$DChC5	460 nm (1035)	595 nm (3130)	0.33	30 min	+475
GRα$_3$DChC5 R24M	465 nm (1090)	595 nm (3410)	0.32	30 min	
GRα$_3$DChC5 R24Y	465 nm (1115)	595 nm (3740)	0.30	30 min	
Nitrosocyanin[14]	390 nm (7000)	490 nm (2200)	3.18		+85[13]
AcNiR[9]	457 nm (2590)	570 nm (1490)	1.74		+240[36]
Stellacyanin[7]	448 nm (1150)	604 nm (4000)	0.29		+184[11]
Plastocyanin[6]	460 nm (400)	597 nm (5200)	0.05		+372[37]

Electron Paramagnetic Resonance (EPR) spectra were obtained for GRα$_3$DChC3, GRα$_3$DChC4, and GRα$_3$DChC5 as well as its R24Y variant at pH 7.5. The EPR spectrum of GRα$_3$DChC3 was fit with a single Cu(II) center with expanded $A_\parallel$ compared to the parent GRα$_3$DChC2 protein. EPR spectra of GRα$_3$DChC4, GRα$_3$DChC5, and GRα$_3$DChC5 R24Y required two Cu(II) centers to properly fit the data (Figure 2). For all three constructs one Cu(II) species has $g_\parallel = 2.24$ and $A_\parallel = 22 \times 10^{-4}$ cm^{-1}. This highly compressed hyperfine coupling constant is reminiscent of that of stellacyanin (Table 2), and may be indicative of tetrahedral geometry.[38] The second EPR site of these three constructs has a $g_\parallel = 2.20$ and $A_\parallel = 166 \times 10^{-4}$ cm^{-1}. The hyperfine coupling in this second EPR site is uncompressed, unlike that of blue or green cupredoxins plastocyanin or CuNiR (Table 2). These two sites are in a roughly 60:40 ratio. Spectra and fits including both components are available in the Supporting Information (SI).

Table 2. Electron Paramagnetic Resonance Fits for Constructs Reported Compared to Native Proteins and GRα$_3$DChC2a

construct	$g_{\|}$	$g_{\|}$	$A_{\|}$ ($\times 10^{-4}$ cm^{-1})	$A_{\perp}$ ($\times 10^{-4}$ cm^{-1})	% of signal	line widths
GRα$_3$DChC2[31]	2.21	2.03	148			
GRα$_3$DChC3	2.139	1.955	164	3		0.04, 0.015, 0.02
GRα$_3$DChC4	[a]2.24	[a]2.09, 2.01	[a]13	[a]10	[a]59	[a]0.012, 0.02, 0.02
	[b]2.25	[b]2.05, 2.00	[b]150	[b]7	[b]41	[b]0.03, 0.01, 0.06
GRα$_3$DChC5	[a]2.25	[a]2.08, 2.01	[a]23	[a]10	[a]61	[a]0.01, 0.02, 0.017
	[b]2.21	[b]2.04, 2.00	[b]167	[b]10	[b]39	[b]0.01, 0.012, 0.02
GRα$_3$DChC5 R24Y pH 7.5	[a]2.24	[a]2.09, 2.02	[a]22	[a]10	[a]61	[a]0.01, 0.015, 0.012
	[b]2.22	[b]2.05, 1.98	[b]167	[b]10	[b]39	[b]0.04, 0.02, 0.035
GRα$_3$DChC5 R24Y pH 5.5	2.28	2.04, 2.02	167	10		0.03, 0.018, 0.024
GRα$_3$DChC5 R24Y pH 7.5 + 3 M NaCl	[a]2.24	[a]2.09, 2.02	[a]22	[a]10	[a]67	[a]0.01, 0.015, 0.012
	[b]2.22	[b]2.05, 1.98	[b]167	[b]10	[b]33	[b]0.04, 0.02, 0.035
GRα$_3$DChC5 R24Y pH 10.0	2.22	2.05, 1.98	167	10		0.03, 0.02, 0.035
Nitrosocyanin[14]	2.245	2.059, 2.036	130	23		
AcNiR[9]	2.195	2.04	73			
Stellacyanin[7]	2.287	2.025, 2.077	35	57, 29		
Plastocyanin[6]	2.226	2.042, 2.059	63			

[a]Superscripts "a" and "b" denote the differing parameters for the two species necessary to simulate the EPR data of GRα$_3$DChC4, GRα$_3$DChC5, and GRα$_3$DChC5 R24Y.

EPR spectra of GRα$_3$DChC5 R24Y were obtained at pH 5.5, 6.5, 7.5, 9.0, and 10.0 as well as varying concentrations of NaCl to explore the pH dependence of the construct's speciation and deconvolute the spectra obtained observed at pH 7.5 (Table 2).

X-ray Absorption Spectroscopy

Cu(I) and Cu(II) forms of GRα$_3$DChC3, GRα$_3$DChC4, and GRα$_3$DChC5 and Cu(II) forms of R24M and R24Y variants of GRα$_3$DChC5 at pH 7.5 were subjected to X-ray Absorption Spectroscopy (XAS) to gain insights into the structural differences between these constructs. The Cu(I) forms of GRα$_3$DChC3, GRα$_3$DChC4, and GRα$_3$DChC5 all have weaker 1s → 4p transitions than that seen for the Cu(I) form of the GRα$_3$DChC2 parent peptide. The intensity of the 1s → 4p transition of Cu(I) XAS has been shown to inversely correlate with the coordination number of Cu(I).[39] Thus, these results indicate an increase in the average Cu(I) coordination number toward more 3-coordinate for Cu(I)GRα$_3$DChC3, Cu(I)GRα$_3$DChC4, and Cu(I)GRα$_3$DChC5 compared to the mixture of 2 and 3 coordinate species assigned to the parent construct Cu(I)GRα$_3$DChC2. EXAFS analyses of the Cu(I) species all exhibit outer-shell scattering typical of His coordination to Cu. Models used to fit the EXAFS data are consistent with a CuHis$_2$S$_1$ binding site for GRα$_3$DChC3, GRα$_3$DChC4, and GRα$_3$DChC5 (Table 3). The fitted Cu(I)–Cys bond distances for all the de novo constructs are around 2.2 Å, similar to that of green and blue cupredoxins but shorter than the 2.3 Å Cu(I)–Cys bond in nitrosocyanin.

Table 3. Cu(I) EXAFS Fitting Parameters of Constructs Reported Compared to Native Cupredoxins

construct	model	Cu–Imid R (Å)	Cu–Imid σ^2 (Å^2) × 10^{-3}	Cu–S R (Å)	Cu–S σ^2 (Å^2) 1 × 10^{-3}
GRα$_3$DChC2[31]	Cu(Imid)$_2$S$_1$	1.92	14.1	2.17	5.8
GRα$_3$DChC3	Cu(Imid)$_2$S$_1$	1.95	18.3	2.20	7.7
GRα$_3$DChC4	Cu(Imid)$_2$S$_1$	1.99	10.7	2.20	7.0
GRα$_3$DChC5	Cu(Imid)$_2$S$_1$	1.97	13.6	2.20	6.0
Nitrosocyanin[14]	Cu(N/O)$_2$S$_1$	1.96	4.0	2.30	3.2
Af Cu nitrite reductase[40a]	Cu(Imid)$_2$S$_1$. . .S$_1$	1.91		2.21	
		2.06		2.41	
Poplar Plastocyanin[41,42]	Cu(Imid)$_2$S$_1$. . .S$_1$	1.96		2.19	
		2.01		2.86	

[a]Distances from EXAFS analysis were not available so those determined crystallographically are shown in the table.

The intensity of the 1s to 3d transition in Cu(II) XAS has been linked to the geometry of the copper site with an increase in tetrahedral character giving an increase in intensity, due to increased 3d+4p mixing.[43,44] Comparing the area of the 1s to 3d transition of our Cu(II) bound constructs we find that GRα$_3$DChC2 has the largest area, and there is a trend of decreasing area as we go from GRα$_3$DChC2 to GRα$_3$DChC3, GRα$_3$DChC4, and GRα$_3$DChC5 and increasing area when GRα$_3$DChC5 is mutated to either R24M or R24Y (Table 4). EXAFS analyses of these Cu(II) species all exhibit long distance scatterers typical of His coordinated to Cu. Models used to fit the EXAFS data are consistent with CuHis$_2$S$_1$ for all constructs reported. Cu(II)–Cys distances for the de novo constructs varied between 2.26 Å for GRα$_3$DChC4 being the longest and 2.20 Å for GRα$_3$DChC5 R24M. These distances are between that of green cupredoxins (2.22 Å) and red cupredoxin (2.30 Å), and longer than those of perturbed blue (2.17 Å) and fully blue cupredoxin (2.08 Å) (Table 4).

Table 4. Cu(II) EXAFS Fitting Parameters of Constructs Reported Compared to Native Cupredoxins

construct	model	Cu–Imid R (Å)	Cu–Imid σ^2 (Å^2) × 10^{-3}	Cu–S R (Å)	Cu–S σ^2 (Å^2) × 10^{-3}	Cu–O R (Å)	Cu–O σ^2 (Å^2) × 10^{-3}	1s to 3d peak area
GRα$_3$DChC2[31]	Cu(Imid)$_2$S$_1$O$_1$	1.97	3.3	2.23	10.6	1.96	7.7	14
GRα$_3$DChC3	Cu(Imid)$_2$S$_1$	1.99	9.90	2.18	13.1			12
GRα$_3$DChC4	Cu(Imid)$_2$S$_1$	1.92	7.6	2.25	9.5			10
GRα$_3$DChC5	Cu(Imid)$_2$S$_1$	1.93	6.0	2.26	9.1			8
GRα$_3$DChC5 R24Y	Cu(Imid)$_2$S$_1$	1.96	7.2	2.22	9.6			13
GRα$_3$DChC5 R24M	Cu(Imid)$_2$S$_1$	1.96	8.6	2.20	5.4			12
Nitrosocyanin[14]	Cu(N/O)$_3$S$_1$	1.96	5.8	2.30	3.2			
Af Cu nitrite reductase[10a]	Cu(Imid)$_2$S$_1$. . .S$_1$	2.07		2.22				
		2.06		2.48				
C.s. Stellacyanin[8]	CuN$_2$S$_1$	1.96	2.5	2.17	4.1			
Poplar Plastocyanin[5]	Cu(N)$_2$S$_1$. . .S$_1$	1.98		2.08				

[a]Distances from EXAFS analysis were not available, so those determined crystallographically are shown in the table.

Discussion

The de novo creation of the constrained metal binding site of a blue copper protein has been a long-standing goal of the de novo metalloprotein community. An ideal de novo recreation of a blue copper protein would have a $\varepsilon_{\sigma/\pi} < 0.5$, a parallel hyperfine coupling constant compressed below 100×10^{-4} cm^{-1}, short Cu(I/II)–S distances of 2.1–2.2 Å, and a reduction potential of 300–400 mV vs NHE. Several groups have successfully created de novo cupredoxins with green copper protein-like spectroscopic properties ($\varepsilon_{\sigma/\pi} \approx 1$) using a variety of different methods.[25−27] Hellinga used a library design method which culminated in a green copper protein-like optical absorption spectrum in the presence of exogenous ligands such as azide ($\varepsilon_{\sigma/\pi} = 0.95$).[25] Lu and Valentine utilized protein redesign of CuZn superoxide dismutase to produce a green copper protein-like site without the need of exogenous ligands ($\varepsilon_{\sigma/\pi} = 1.02$) and a compressed hyperfine coupling constant below 15×10^{-4} cm^{-1}.[26] Finally, Schnepf and Hildebrandt utilized a library of four helix bundle peptides to create a green copper protein with $\varepsilon_{\sigma/\pi} \approx 1$ but the parallel hyperfine coupling constant remained uncompressed at 123×10^{-4} cm^{-1}.[27] Recently, two groups have successfully recreated blue copper protein spectroscopic properties, but both required exogenous ligands to do so. Mann and Borovik used a cysteine containing variant of streptavidin with a series of biotinylated copper complexes to produce a Cu(II) site with $\varepsilon_{\sigma/\pi} = 0.29$, $A_{\parallel} = 23 \times 10^{-4}$ cm^{-1}, an apparent reduction potential of 110 mV vs NHE, and a short Cu(II)–S distance of 2.11 Å.[45] Shiga and Tanaka rationally designed a de novo green copper protein within a four helical bundle which can be tuned to give blue copper protein-like spectroscopic properties ($\varepsilon_{\sigma/\pi} = 0.34$, $A_{\parallel} = 17 \times 10^{-4}$ cm^{-1}), apparent reduction potential (328 mV vs NHE), and geometry (Cu(II)–S distance which the authors describe as on the longer end of the blue copper protein range at 2.30 Å) with high concentrations of an exogenous ligand such as Cl^-.[28,29] These successes reflect significant progress, but the goal of a self-contained de novo blue copper protein still remained. Several significant questions still needed answering, such as whether there were certain design elements present in the native system (such as backbone carbonyl to Cu(II) interactions) that were required, but unavailable within an alpha helical scaffold.

Our laboratory recently reported a de novo red cupredoxin with spectroscopic properties reminiscent of either blue Cu protein variants M148E rusticyanin and M121E azurin or the native red Cu protein nitrosocyanin.[12−14,22,30] Further investigation of this site through site directed mutagenesis determined that a Cu–Glu41 interaction not included in the design led to this red Cu protein site.[31] Mutation of Glu41 to Gln or Ala did not create a blue Cu protein, leading us to conclude that our site was best described as a nitrosocyanin-like model rather than a blue Cu protein variant. Given this new understanding of our construct, we sought alternative strategies previously applied to native systems to tune the spectroscopic properties of our construct from red to green or blue.

GRα$_3$DChC3 and GRα$_3$DChC4 Design and Cu(II) Spectroscopy

The design of GRα$_3$DChC3 and GRα$_3$DChC4 was based on an inversion of the metal binding site, which has recently been reported as a strategy to convert the Cu(II) binding geometry of the blue Cu protein azurin to that of the red Cu protein nitrosocyanin through M121H H46E mutations.[23] GRα$_3$DChC3 and GRα$_3$DChC4 reverse the strategy used on azurin in one of two possible ways. GRα$_3$DChC3 uses an H38M E41H inversion to create a MxxH chelation motif and leave Cys21 and His25 in a CxxxH motif while GRα$_3$DChC4 contains an H25M E41H inversion with HxxH and CxxxM chelation motifs. Cu(II) addition to these peptides shows that these two strategies are not equivalent. GRα$_3$DChC3 exhibits a noncupredoxin-like copper thiolate spectrum with higher $\varepsilon_{\sigma/\pi}$ than the parent construct (3.8) and expanded hyperfine coupling constant of 164×10^{-4} cm^{-1}. GRα$_3$DChC4 has spectroscopic properties reminiscent of a green copper protein with red-shifted Cu–Cys π LMCT (from 490 to 600 nm), a lower

$\varepsilon_{\sigma/\pi}$ (0.87) than its parent, and an EPR spectrum composed of multiple species, one of which contains a compressed hyperfine coupling constant. (Figure 3 and Tables 1 and 2)

On the basis of the crystal structure of the scaffold protein GRα_3D, we believe the reason for the different optical absorption spectra of these two mutation strategies (GRα_3DChC3 and GRα_3DChC4) is whether or not all three designed primary sphere amino acids (His_2Cys) are able to coordinate well to the Cu. The original structure of GRα_3DChC2 has a His_2Cys site at positions C21, H25, and H38, all of which would have β carbons within 8 Å of one another based on the scaffold GRα_3D crystal structure. The β carbon of the Glu41 position is a full 12 Å from His25, but the longer and more flexible nature of Glu41 allows all four residues to interact with the Cu center. When one His is moved to the 41 position to invert the binding site the remaining His residue of the His_2Cys binding site can be at either position 38 (5 Å away) or position 25 (12 Å away). On the basis of the spectroscopic differences between GRα_3DCChC3 and GRα_3DChC4 we conclude that having the two His residues 12 Å apart does not allow both to strongly ligate the Cu(II) simultaneously. This is consistent with the increased Debye-Waller factors for the Cu–N(His) shell for GRα_3DChC3 fits in both Cu(I) and Cu(II) oxidation states as determined by XAS. Similar spectra were observed for H46G and H117G mutants of azurin, showing that losing the His_2Cys ligation sphere can result in a type 2 Cu–thiolate spectrum.[46,47] This analysis using the scaffold crystal structure is only reasonable if the distances between the β carbons in the mutated construct and its Cu(II) bound variant remain roughly the same as those in the original crystal structure. If there are any large changes to the structure from either of these effects, then other explanations of the success of GRα_3DChC4 compared to GRα_3DCChC3 would be necessary.

Having successfully created a de novo green cupredoxin we tested whether or not our construct could use exogenous ligands to tune its optical absorption spectrum to that of a blue copper protein, similar to the construct created by Shiga and Tanaka.[28] We determined that adding a large excess of NaCl (1 M) red shifts the higher energy transition from 410 to 475 nm and decreases the intensity ratio from 0.87 to 0.46. These values are very similar to a perturbed blue copper protein such as stellacyanin (Table 1). Our proposed causes of this effect are discussed below.

GRα_3DChC5 and Variant Designs and Cu(II) Spectroscopy

We next sought to tune the green copper protein spectroscopic properties of GRα_3DChC4 to those of a blue copper site using mutation rather than an exogenous ligand to create the first self-contained de novo blue cupredoxin. The delicate nature of this conversion was recently exemplified in artificial metalloproteins based on a biotin streptavidin system where a single methyl group addition to the complex tuned the resulting Cu(II) complex from exhibiting the spectroscopic properties of a green copper protein to that of a blue copper protein.[45] Mutation studies of native cupredoxins have successfully converted a green cupredoxin to blue by decreasing the strength of the axial amino acid in M182T Cu nitrite reductase.[20,21] This follows the "coupled distortion" model based on structure comparisons of green and blue cupredoxins, in which the increased Cu–Met bond distance is coupled to a decreased Cu–Cys bond distance as one goes from green to perturbed blue and finally blue copper proteins.[3] We created GRα_3DChC5 (GRα_3DChC2 H25I E41H) using a similar tactic to mutate out the axial interaction in GRα_3DChC4 (Figure 4). Comparing GRα_3DChC5 to GRα_3DChC4 we see that taking out the presumed axial interaction (via M25I mutation) shifts the higher energy absorption band from 410 to 460 nm and increases the intensity of the 595 nm transition, and in this way, decreases the ratio of these bands to 0.33. This results in a spectrum that is reminiscent of perturbed blue copper proteins such as stellacyanin or the M182T variant of CuNiR. Thus, we have successfully created red copper (GRα_3DChC2), green copper (GRα_3DChC4), and perturbed blue copper protein (GRα_3DChC5) metal binding sites within the same de novo scaffold using rational design.

Finally, we created several variants of GRα_3DChC5 by mutating Arg24 to either Met or Tyr, to test the effect of mutations at this site. This residue should orient its side chain close to the metal binding site created by His41, His38, and Cys21. Both R24M and R24Y mutations create constructs with very similar optical absorption spectra with transition intensity ratios of 0.32 and 0.30, respectively. We have previously shown that a Tyr can be a useful amino acid for electron hopping to improve intramolecular electron transfer rates, so knowing that a Tyr can be positioned so close to the metal binding site without significant perturbation will be important for future studies.[48]

Deconvoluting Cu(II) Binding Species

While optical absorbance spectra of our Cu(II) bound GRα_3DChC4 and GRα_3DChC5 constructs indicated we had successfully recreated green and blue cupredoxins within our de novo scaffolds, the multiple species apparent in EPR required explanation. Most cupredoxins are exceptionally stable to pH changes with minimal effects to their Cu(II) optical absorption and EPR spectra such as the cases of stellacyanin and pseudoazurin.[49–51] However, the presence of two spin systems has previously been observed for the azurin variant C112D/M121E due to protonation equilibria of the active site His35.[52] Therefore, we explored the pH dependence of our green and blue copper proteins by characterizing GRα_3DChC4 at pH 5.5, 6.5, 7.5, 9.0, and 10.0 by optical absorption spectroscopy while GRα_3DChC5 R24Y was characterized at those same pH conditions using EPR and optical absorption spectroscopies.

Increasing the pH from 7.5 to 10.0 biases the optical absorption spectrum toward a site with a LMCT at 390 nm but no absorption bands of lower energy, while the ratio of species observed by EPR biases toward the spin center with $A_{\parallel}$ = 167 (Figures 5 and S16). This is consistent with the Cu(II) maintaining its Cu–S bond at higher pH but losing the constrained blue copper geometry. Decreasing pH from 7.5 down to 5.5, the optical absorption spectral intensity of all LMCT signals decreases indicating the Cu–S bond is lost while the EPR spectrum biases toward a third spin system not present at neutral pH (Figures 5 and S17). The two species observed in EPR at pH 7.5 are affected by pH, but we were unable to use decreased pH to bias the system toward the desired blue copper protein binding geometry. Our results are consistent with Cys protonation at lower pH causing a loss of Cu–S binding, but one would also expect a loss of salt bridge interactions within our scaffold as we approach the pK_a of Glutamate, which would cause tertiary structure changes. The combination of these factors complicates analysis. Circular Dichroism analysis indicates that the protein does not denature appreciably at extreme pH but this can only report on loss of secondary structure (Figure S20). Similarly, at higher pH one would also expect a loss of salt bridge interactions as we approach the pK_a of Arginine, which would allow the scaffold to rearrange and lose the desired constrained geometry of a blue copper protein.

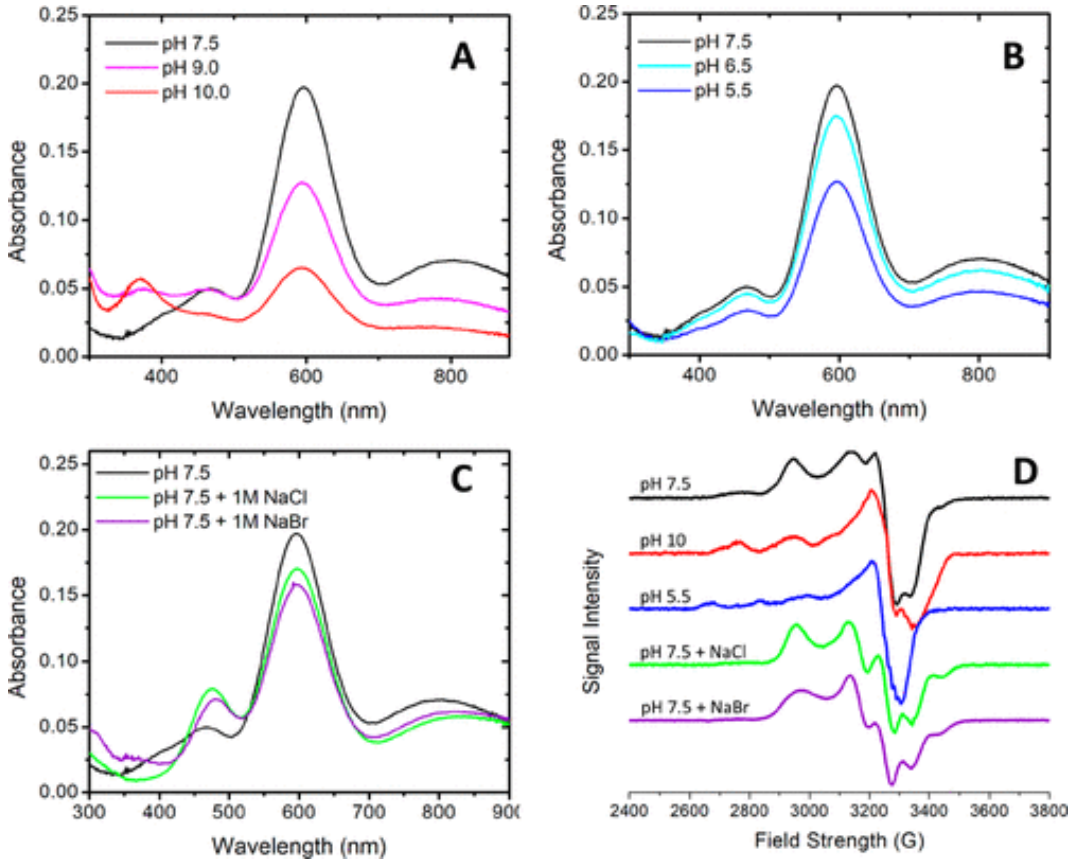

Figure 5. Optical absorption spectra of 50 µM Cu(II) with 75 µM GRα_3DChC5 R24Y showing the effects of increasing pH (A), decreasing pH (B), and excess salt (C) as well as EPR spectra of 500 µM Cu(II) with 750 µM GRα_3DChC5 R24Y under the most illustrative conditions (D). EPR spectra were recorded using CW X-band collected at 9.30 MHz, 100 K, and 20.51 mW microwave power.

We next tested whether our constructs could use exogenous ligands to tune their spectroscopy similar to the construct created by Shiga and Tanaka, which appears green until high concentrations of NaCl or other presumptive ligands are added.[28,29] The ability to bind exogenous ligands is interesting, as native cupredoxins rarely bind exogenous ligands unless a metal coordinating residue is removed such as the His117,[46,53,54] Met121,[55,56] and His46[47] mutants of azurin. Recent investigations with model compounds and a nitrosocyanin-like azurin mutant have hinted at a possible mechanism for NO binding to blue copper proteins but this has not yet been observed for native blue copper proteins.[23,57,58]

The addition of molar concentrations of NaCl to either GRα_3DChC4 or GRα_3DChC5 R24Y results in a species with a blue copper protein-like optical absorption spectrum with bands at 475 and 600 nm and an intensity ratio of 0.4 similar to the perturbed blue copper protein stellacyanin (Table 1 and Figures 3 and 5). The stability of the Cu(II) signal is also impacted with Cu(II) signal roughly doubling in half-life compared to in the absence of NaCl (50 min compared to 15–30 min for constructs without NaCl present). Interestingly, when molar concentrations of NaCl were added to GRα_3DChC5 R24Y the EPR indicates that this biases slightly toward the compressed hyperfine coupling spin system that was already present at neutral pH (Tables S9 and S10). We have also determined that the same changes are seen with molar concentrations of NaBr in both optical absorption and EPR spectroscopy, and that at least 10 mM NaCl is necessary to see the spectral changes detailed above (Figures S18 and S19). Given all of these factors, we conclude that the effect of high concentrations of NaCl is not due to binding to copper, but due to other effects of high salt concentration on the Cu(II) active site. High concentrations of NaCl can act as a kosmotrope as part of the Hofmeister series, improving protein

stability and in some cases improving kinetic parameters.[59,60] We propose that this improved stability is allowing the construct to bias the equilibrium observed by EPR toward the more constrained blue copper binding site geometry, but even in the presence of 3 M NaCl the system is only 67% in the desired geometry based on EPR.

An obvious question arises: why was the Cu(II) bound state of our de novo red cupredoxin (GRα_3DChC2) a single species based on all evidence when EPR indicates both our green and blue cupredoxins are mixtures? We propose that this difference is linked to the rearrangement required to convert from red to green/blue. Repositioning of one of the binding His residues from inside the helical bundle at position 25 to the helical interface position 41 has several consequences (Figure 3). His is shorter than Glu which would likely require a repositioning of the bound Cu(II) closer to the helical interface. This makes the metal more solvent exposed allowing water access to the Cu(II) environment which could be related to the much shorter half-lives seen for these constructs compared to the original GRα_3DChC2 (Table 1). Repositioning His near the helical interface could also allow that residue to hydrogen bond with the solvent or nearby surface residues. This would be consistent with the pH dependent nature of these two spin states.

Structural Insights from Cu(II) XAS Compared to Native Cupredoxins

Using EXAFS, it is informative to compare the average Cu(II) bond distances of our de novo series of cupredoxins to those of native cupredoxins to discern if patterns observed in native cupredoxins are also observed within de novo cupredoxins. The general trend within the series of red to green to blue natural cupredoxins is a decreasing Cu–S distance (Table 4). Trends between blue and green cupredoxins in nature have led to a coupled distortion model. The series from green to blue cupredoxins has a decreased axial interaction (increase in distance) and decreased Cu(II)–Cys distance, leading to a rotation of the Cu $d_{x^2-y^2}$ orbital to align more with the Cys π-donor MO than with the σ-donor orbital. This rotation decreases the $\varepsilon_{\sigma/\pi}$ ratio and changes the optical absorption spectra from a green to blue copper protein.[3] While the red copper protein nitrosocyanin's active site is not as directly comparable as those of green and blue copper proteins it is interesting that this general trend of decreasing Cu–S distance as the $\varepsilon_{\sigma/\pi}$ decreases is maintained. Comparing the same series within our de novo constructs is complicated by the mixed nature of the blue (GRα_3DChC5) and green (GRα_3DChC4) cupredoxins compared to our original red construct (GRα_3DChC2) which showed no indication of multiple spin states. Taking into account that GRα_3DChC4 and GRα_3DChC5 exist as a 60:40 ratio of type 1 and type 2 copper centers we can estimate the distance of a pure type 1 GRα_3DChC4 or GRα_3DChC5 if one assumes a typical type 2 Cu–S distance of 2.30 Å. This would give Cu–S distances of 2.22 Å for pure GRα_3DChC4, 2.23 Å for pure GRα_3DChC5, and 2.17 Å for pure GRα_3DChC5 R24Y. Using this analysis the Cu–S distance of 2.23 Å of GRα_3DChC2 (our red cupredoxin) is surprisingly similar to that of our blue and green cupredoxins.

Comparisons between our green and blue cupredoxins can be done directly because they all exist in the same mixed state of 60% type 1 and 40% type 2. It is interesting to note that while the trend within native systems has decreasing Cu–S distance between a green site like AfCuNiR (2.22 Å) and a perturbed blue site like stellacyanin (2.17 Å) our constructs have indistinguishably similar average bond distances between green (GRα_3DChC4) and perturbed blue copper centers (GRα_3DChC5). (Table 4) EXAFS comparisons of WT and M182T AfCuNiR are unfortunately unavailable for a more direct comparison to our data, but previous studies indicated that the Cu(II)–Cys bond was stronger in M182T compared to WT based on resonance Raman spectroscopy of the Cu(II)–S(Cys) stretching frequency.[20] This assignment was reconfirmed more recently when investigating the temperature dependent interaction of Met182 with the Cu center.[61] Our EXAFS studies, however, do not follow this overarching trend.

This deviation from the coupled distortion model is also apparent when looking at further blue cupredoxins with R24X mutations (Table 4). We find that the average Cu–S distance can vary significantly within the series of GRα_3DChC5 "WT", R24Y, and R24M, from 2.26 to 2.20 Å, although the optical absorption and EPR spectra remain largely invariant. Although strategies based on the coupled distortion model allowed us to recapitulate green and blue optical absorption spectroscopic properties within a de novo construct, the correlation of Cu(II)–Cys bond strength to the optical absorption profile does not hold in our alpha helical scaffold. Recently, several green cupredoxins have been discovered that do not include the complication of a second type 2 copper site within the same protein.[62−65] EXAFS studies of WT and axial mutation variants of these new cupredoxins will be an important addition to our understanding of how structure dictates optical absorption spectroscopic properties in green copper proteins.

Cu(I) Geometry and Apparent Reduction Potentials

Combining this work with our previously published de novo cupredoxins we find that the Cu(I) geometry and apparent reduction potentials of these constructs change upon conversion from red copper protein (GRα_3DChC2) to green/blue (GRα_3DChC4 and GRα_3DChC5), but that among green/blue constructs there is little change.[30,31] The Cu(I)–Cys distance of GRα_3DChC2 was previously reported as 2.17 Å, a value more consistent with natural green/blue copper proteins than a red copper protein (Table 3). Repositioning of the metal binding His from the hydrophobic core at position 25 to the helical interface at position 41 increases the Cu(I)–Cys distance to 2.20 Å. This is even observed in constructs which did not reproduce cupredoxin Cu(II) spectroscopic properties (GRα_3DChC3). We propose that this increase in Cu(I)–Cys distance is due to the decreased side chain length of His41 compared to Glu41.

Across this series of E41H constructs (GRα_3DChC3, GRα_3DChC4, and GRα_3DChC5) we find the Cu(I)–Cys distance is consistently 2.20 Å regardless of the structural modification of the Cu(II) bound variant. That this distance has remained within the relatively narrow range of 2.16 to 2.23 Å, even for constructs that have red copper or normal copper-like spectra, might indicate that the scaffold itself is somehow a factor in maintaining consistent Cu(I) geometries. We propose that the location of the copper coordinating ligands within our 3HB scaffold is too inflexible and prevents gross reorientation of some of the copper ligand environment, even with significant modification to the primary coordination sphere. These interactions could explain the invariance of our measured electrochemical potentials for constructs with significantly different spectroscopic features.

A similar pattern is observed when looking at Cu apparent reduction potentials within our scaffolds where the jump from GRα_3DChC2 to GRα_3DChC4 and GRα_3DChC5 comes with a measurable shift from +530 mV to +475 mV. This shift is likely linked to the multiple species (60% type 1, 40% type 2) observed by EPR in GRα_3DChC4 and GRα_3DChC5, but not in GRα_3DChC2. This shift is opposite to that observed in native red and green copper proteins which increase from +57 mV to +157 mV. We propose that repositioning of the Cu binding His from position 25 to 41 between these constructs pulls the Cu closer to the helical interface and creates a less hydrophobically buried binding site. The change in apparent reduction potential could also be explained by increased access of His41 to hydrogen bonding interactions from solvent.

Comparing GRα_3DChC4 and GRα_3DChC5 it is interesting to note that a significant change in Cu(II) spectroscopic properties has not been met with any change in apparent reduction potential. When similar mutations are applied in CuNiR, the apparent reduction potential is shifted from +147 to +250 mV, consistent with results across a range of blue copper proteins.[21,41] We believe the same factors are at play with these mutations within our constructs as what led to the shift in potential discussed above. These discrepancies between native cupredoxins and our de novo designs may be related to

our choice of scaffold, as we see a similar narrow range of apparent reduction potentials when results for CuNiR based Type 2 $CuHis_3$ sites within the 3SCC scaffold TRI are included.[66–68] All of these constructs fall within the relatively narrow range of 300–500 mV at pH 7.5 or 400–600 mV at pH 5.8, even when non-native amino acids such as methylated histidine are included. Native copper proteins, however, have apparent reduction potentials within a much larger range, with cupredoxins ranging from +85 mV in nitrosocyanin[13] to +184 and +308 mV for stellacyanin[11] and azurin[69] all the way to +580 mV for rusticyanin,[12] all within the cupredoxin fold.

Protein redesign efforts with azurin have shown that tuning hydrophobicity and hydrogen-bonding interactions within the secondary sphere can tune the apparent reduction potential of that construct over a range of 700 mV.[70] Similar strategies have been attempted within three stranded coiled-coil Cu nitrite reductase constructs which can shift the apparent reduction potential up to 100 mV by increasing or decreasing the prevalence of charged residues near the bound Cu, but getting beyond that 100 mV range may prove difficult.[67] Exclusion of solvent and introduction of hydrogen bonding interactions to the Cys bound to Cu have been shown to increase apparent reduction potentials within cupredoxins and (in the case of solvent exclusion) other redox metal centers as much as +200 mV.[71]

Implications for Future Designs

We have successfully created a blue copper protein by realizing that reorientation of the active site in a way similar to what has been done in native blue copper proteins can lead to a successful design. Simply adding the appropriate residues in a hydrophobic core allowed for a design that recapitulated a red copper protein. Only after realizing that the surface amino acid Glu41 was interacting directly with the bound Cu(II) were we able to rotate the active site to develop a green/blue cupredoxin from the original red scaffold. While this is a major step forward within the metalloprotein design arena, we were unable to achieve more than 60% type 1 copper without the addition of additives like NaCl. The pH dependence studies indicate that the amount of the species with a blue copper geometry diminishes when pH differs from neutral. This is not the case in native blue copper proteins whose Cu(II) spectra are often remarkably stable to pH changes.[49–51] This complicated and tenuous system of equilibria in our constructs could be related to the sluggish electron transfer we observe which is likely due to increased reorganization energies. We also find that the Cu(II) signal of $GR\alpha_3DChC4$ and $GR\alpha_3DChC5$ is more quickly bleached than the original $GR\alpha_3DChC2$. Both of these observations, sluggish electron transfer and instability of the center, suggest that future designs to make functional type 1 copper proteins will require movement of the Cu from the protein periphery into the hydrophobic core.

Our most successful cupredoxin models incorporated binding sites spanning only two of the possible three helices of $GR\alpha_3D$. Creating constructs which span all three helices of the scaffold should be a focus of further designs. This repositioning will better exclude the metal binding site from surrounding solvent and, as a side benefit, improve the efficacy of hydrophobic core repacking strategies. Recently Polizzi and DeGrado published a study in which hydrophobic core repacking of the protein around a Zn porphyrin was used to create a hyperstable protein–ligand complex.[72] We hypothesize that a de novo blue copper protein with a buried metal binding site using this hydrophobic core repacking strategy would produce a more stable and functional type 1 copper protein model.

An alternative strategy for improving the stability of our constructs is to increase the length of the scaffold in a similar fashion to what we have previously reported.[31] Initial results with a less thermodynamically stable α_3DChC5 indicate decreased blue copper protein character and a much lower Cu(II) site half-life of less than 1 min (Figure S21). One might expect stabilizing the scaffold beyond that of $GR\alpha_3DChC5$ to have the opposite effect, but the comparison of Cu(II) metal site stability within $GR\alpha_3DChC2$ to $GR\alpha_3DChC4$ and $GR\alpha_3DChC5$ would indicate that this strategy will not work

alone. An optimal strategy will still require metal binding site repositioning toward the protein's hydrophobic core.

We have previously shown that Cu bound constructs using our alpha helical bundle or three stranded coiled coil scaffolds all have apparent reduction potentials falling within a relatively small range of 300–500 mV. We propose that the flexibility of our scaffolds does not create the hydrophobic environment needed for large changes to the apparent reduction potential of the bound metal. We hypothesize that larger scaffolds which exclude solvent better would allow for Cu centers in which one can drastically tune their apparent reduction potential similar to native cupredoxins (Table 1). For example, three stranded coiled coils designed by the Baker laboratory to incorporate hydrogen bonding with concentric rings of alpha helical bundles may exclude solvent enough to allow for greater flexibility in apparent reduction potential of bound Cu within a three stranded coiled-coil construct.[73]

Conclusions

Recreation of strained metal binding sites within de novo scaffolds has long been a goal of the metalloprotein design community as it showcases the ability of proteins to enforce nonpreferred metal geometries to produce unique spectral and geometric properties. Cupredoxins are arguably the prototypical strained metal binding sites with red, green and blue variants, with blue copper proteins sitting atop the proverbial strained metal binding site throne. The differentiating factors of these sites center around the Cu–S bond which leads to unique optical absorption ($\varepsilon_{\sigma/\pi} > 2$ for red, $\varepsilon_{\sigma/\pi} \approx 1$ for green, and $\varepsilon_{\sigma/\pi} < 0.5$ for blue) and EPR ($A_{\parallel} > 100 \times 10^{-4}$ cm^{-1} for red and $A_{\parallel} < 100 \times 10^{-4}$ cm^{-1} for green/blue) spectra stemming from the Cu–S geometry (Cu–S = 2.3 Å for red and Cu–S = 2.1–2.2 Å for green/blue). Several research groups have previously attempted to recreate the spectral properties of a blue copper protein within a noncupredoxin fold, but successful creation of blue copper spectroscopic properties have invariably required exogenous ligands.[28,29,45]

In this work, we focused our attention on a previously reported red copper protein ($\varepsilon_{\sigma/\pi} = 2.33$, $A_{\parallel} = 148 \times 10^{-4}$ cm^{-1}) and, through rational design, have successfully tuned this construct to green ($\varepsilon_{\sigma/\pi} = 0.87$, $A_{\parallel} = 13 \times 10^{-4}$ cm^{-1}) and blue copper protein sites, with corresponding spectroscopic properties ($\varepsilon_{\sigma/\pi} = 0.33$, $A_{\parallel} = 22 \times 10^{-4}$ cm^{-1}). This is the first designed blue copper protein within a noncupredoxin fold, using only amino acid interactions with the bound Cu(II). While the strategies used to create these new constructs were based off mutation studies of native cupredoxins, our series of de novo cupredoxins have some striking differences to native constructs. The coupled distortion model in which green to blue cupredoxins have progressively shorter and, therefore, stronger Cu(II)–Cys bonds is not observed within our constructs, and de novo blue copper proteins can vary in Cu(II)–Cys bond length from 2.26 to 2.20 Å. EPR investigation into our constructs revealed an equilibrium of metal binding geometries which can be influenced by changing pH or high concentrations of NaCl. Future designs will investigate how the correctly constrained metal geometry can be enforced to improve its stability at various conditions.

Supporting Information

DNA sequences of all genes and amino acid sequences of all proteins used during this study, tables of Cu(I) or Cu(II) EXAFS fitting parameters and figures, figure of EPR fits for electrochemical analysis, and figure of EPR spectra and explanation of analysis.

Acknowledgments

T.B.J.P. acknowledges the Natural Sciences and Engineering Research Council of Canada for support in the form of a Postdoctoral Fellowship. V.L.P thanks the National Institutes of Health for financial support of this research (ES012236). V.S.A. acknowledges a Rackham Merit Fellowship from the

University of Michigan. Use of the Stanford Synchrotron Radiation Lightsource, SLAC National Accelerator Laboratory, is supported by the U.S. Department of Energy, Office of Science, Office of Basic Energy Sciences under Contract No. DE-AC02-76SF00515. The SSRL Structural Molecular Biology Program is supported by the DOE Office of Biological and Environmental Research, and by the National Institutes of Health, National Institute of General Medical Sciences (including P41GM103393). The contents of this publication are solely the responsibility of the authors and do not necessarily represent the official views of NIGMS or NIH.

References

1. Liu, J.; Chakraborty, S.; Hosseinzadeh, P.; Yu, Y.; Tian, S.; Petrik, I.; Bhagi, A.; Lu, Y. Metalloproteins Containing Cytochrome, Iron–Sulfur, or Copper Redox Centers. *Chem. Rev.* **2014**, *114* (8), 4366– 4469.
2. Winkler, J. R.; Gray, H. B. Electron Flow through Metalloproteins. *Chem. Rev.* **2014**, *114* (7), 3369– 3380.
3. Solomon, E. I. Spectroscopic Methods in Bioinorganic Chemistry: Blue to Green to Red Copper Sites. *Inorg. Chem.* **2006**, *45* (20), 8012– 8025.
4. Solomon, E. I.; Hadt, R. G. Recent advances in understanding blue copper proteins. *Coord. Chem. Rev.* **2011**, *255* (7–8), 774– 789.
5. Scott, R. A.; Hahn, J. E.; Doniach, S.; Freeman, H. C.; Hodgson, K. O. Polarized x-ray absorption spectra of oriented plastocyanin single crystals. Investigation of methionine-copper coordination. *J. Am. Chem. Soc.* **1982**, *104* (20), 5364– 5369.
6. Penfield, K. W.; Gay, R. R.; Himmelwright, R. S.; Eickman, N. C.; Norris, V. A.; Freeman, H. C.; Solomon, E. I. Spectroscopic studies on plastocyanin single crystals: a detailed electronic structure determination of the blue copper active site. *J. Am. Chem. Soc.* **1981**, *103* (15), 4382– 4388.
7. Malmström, B. G.; Reinhammar, B.; Vänngård, T. The state of copper in stellacyanin and laccase from the lacquer tree Rhus vernicifera. *Biochim. Biophys. Acta, Bioenerg.* **1970**, *205* (1), 48– 57.
8. DeBeer, S.; Randall, D. W.; Nersissian, A. M.; Valentine, J. S.; Hedman, B.; Hodgson, K. O.; Solomon, E. I. X-ray Absorption Edge and EXAFS Studies of the Blue Copper Site in Stellacyanin: Effects of Axial Amide Coordination. *J. Phys. Chem. B* **2000**, *104* (46), 10814– 10819.
9. LaCroix, L. B.; Shadle, S. E.; Wang, Y.; Averill, B. A.; Hedman, B.; Hodgson, K. O.; Solomon, E. I. Electronic Structure of the Perturbed Blue Copper Site in Nitrite Reductase: Spectroscopic Properties, Bonding, and Implications for the Entatic/Rack State. *J. Am. Chem. Soc.* **1996**, *118* (33), 7755– 7768.
10. Tocheva, E. I.; Rosell, F. I.; Mauk, A. G.; Murphy, M. E. P. Side-On Copper-Nitrosyl Coordination by Nitrite Reductase. *Science* **2004**, *304* (5672), 867– 870.
11. Sailasuta, N.; Anson, F. C.; Gray, H. B. Studies of the thermodynamics of electron transfer reactions of blue copper proteins. *J. Am. Chem. Soc.* **1979**, *101* (2), 455– 458.
12. Hall, J. F.; Kanbi, L. D.; Strange, R. W.; Hasnain, S. S. Role of the Axial Ligand in Type 1 Cu Centers Studied by Point Mutations of Met148 in Rusticyanin. *Biochemistry* **1999**, *38* (39), 12675– 12680.

13. Arciero, D. M.; Pierce, B. S.; Hendrich, M. P.; Hooper, A. B. Nitrosocyanin, a Red Cupredoxin-like Protein from Nitrosomonas europaea. *Biochemistry* **2002**, *41* (6), 1703– 1709.

14. Basumallick, L.; Sarangi, R.; DeBeer George, S.; Elmore, B.; Hooper, A. B.; Hedman, B.; Hodgson, K. O.; Solomon, E. I. Spectroscopic and Density Functional Studies of the Red Copper Site in Nitrosocyanin: Role of the Protein in Determining Active Site Geometric and Electronic Structure. *J. Am. Chem. Soc.* **2005**, *127* (10), 3531– 3544.

15. Slutter, C. E.; Sanders, D.; Wittung, P.; Malmström, B. G.; Aasa, R.; Richards, J. H.; Gray, H. B.; Fee, J. A. Water-Soluble, Recombinant CuA-Domain of the Cytochrome ba3 Subunit II from Thermus thermophilus. *Biochemistry* **1996**, *35* (11), 3387– 3395.

16. Wittung-Stafshede, P.; Hill, M. G.; Gomez, E.; Di Bilio, A. J.; Karlsson, B. G.; Leckner, J.; Winkler, J. R.; Gray, H. B.; Malmström, B. G. Reduction potentials of blue and purple copper proteins in their unfolded states: a closer look at rack-induced coordination. *JBIC, J. Biol. Inorg. Chem.* **1998**, *3* (4), 367– 370.

17. Randall, D. W.; Gamelin, D. R.; LaCroix, L. B.; Solomon, E. I. Electronic structure contributions to electron transfer in blue Cu and CuA. *JBIC, J. Biol. Inorg. Chem.* **2000**, *5* (1), 16– 29.

18. Savelieff, M. G.; Wilson, T. D.; Elias, Y.; Nilges, M. J.; Garner, D. K.; Lu, Y. Experimental evidence for a link among cupredoxins: Red, blue, and purple copper transformations in nitrous oxide reductase. *Proc. Natl. Acad. Sci. U. S. A.* **2008**, *105* (23), 7919– 7924.

19. Hosseinzadeh, P.; Tian, S.; Marshall, N. M.; Hemp, J.; Mullen, T.; Nilges, M. J.; Gao, Y.-G.; Robinson, H.; Stahl, D. A.; Gennis, R. B.; Lu, Y. A Purple Cupredoxin from Nitrosopumilus maritimus Containing a Mononuclear Type 1 Copper Center with an Open Binding Site. *J. Am. Chem. Soc.* **2016**, *138* (20), 6324– 6327.

20. Basumallick, L.; Szilagyi, R. K.; Zhao, Y.; Shapleigh, J. P.; Scholes, C. P.; Solomon, E. I. Spectroscopic Studies of the Met182Thr Mutant of Nitrite Reductase: Role of the Axial Ligand in the Geometric and Electronic Structure of Blue and Green Copper Sites. *J. Am. Chem. Soc.* **2003**, *125* (48), 14784– 14792.

21. Olesen, K.; Veselov, A.; Zhao, Y.; Wang, Y.; Danner, B.; Scholes, C. P.; Shapleigh, J. P. Spectroscopic, Kinetic, and Electrochemical Characterization of Heterologously Expressed Wild-Type and Mutant Forms of Copper-Containing Nitrite Reductase from Rhodobacter sphaeroides 2.4.3. *Biochemistry* **1998**, *37* (17), 6086– 6094.

22. Karlsson, B. G.; Tsai, L.-C.; Nar, H.; Sanders-Loehr, J.; Bonander, N.; Langer, V.; Sjölin, L. X-ray Structure Determination and Characterization of the Pseudomonas aeruginosa Azurin Mutant Met121Glu. *Biochemistry* **1997**, *36* (14), 4089– 4095.

23. Tian, S.; Liu, J.; Cowley, R. E.; Hosseinzadeh, P.; Marshall, N. M.; Yu, Y.; Robinson, H.; Nilges, M. J.; Blackburn, N. J.; Solomon, E. I.; Lu, Y. Reversible S-nitrosylation in an engineered azurin. *Nat. Chem.* **2016**, *8*, 670– 677.

24. Yu, F.; Cangelosi, V. M.; Zastrow, M. L.; Tegoni, M.; Plegaria, J. S.; Tebo, A. G.; Mocny, C. S.; Ruckthong, L.; Qayyum, H.; Pecoraro, V. L. Protein Design: Toward Functional Metalloenzymes. *Chem. Rev.* **2014**, *114* (7), 3495– 3578.

25. Hellinga, H. W. Construction of a Blue Copper Analogue through Iterative Rational Protein Design Cycles Demonstrates Principles of Molecular Recognition in Metal Center Formation. *J. Am. Chem. Soc.* **1998**, *120* (39), 10055– 10066.

26. Lu, Y.; LaCroix, L. B.; Lowery, M. D.; Solomon, E. I.; Bender, C. J.; Peisach, J.; Roe, J. A.; Gralla, E. B.; Valentine, J. S. Construction of a blue copper site at the native zinc site of yeast copper-zinc superoxide dismutase. *J. Am. Chem. Soc.* **1993**, *115* (14), 5907– 5918.

27. Schnepf, R.; Haehnel, W.; Wieghardt, K.; Hildebrandt, P. Spectroscopic Identification of Different Types of Copper Centers Generated in Synthetic Four-Helix Bundle Proteins. *J. Am. Chem. Soc.* **2004**, *126* (44), 14389– 14399.

28. Shiga, D.; Nakane, D.; Inomata, T.; Funahashi, Y.; Masuda, H.; Kikuchi, A.; Oda, M.; Noda, M.; Uchiyama, S.; Fukui, K.; Kanaori, K.; Tajima, K.; Takano, Y.; Nakamura, H.; Tanaka, T. Creation of a Type 1 Blue Copper Site within a de Novo Coiled-Coil Protein Scaffold. *J. Am. Chem. Soc.* **2010**, *132* (51), 18191– 18198.

29. Shiga, D.; Hamano, Y.; Kamei, M.; Funahashi, Y.; Masuda, H.; Sakaguchi, M.; Ogura, T.; Tanaka, T. Tuning the geometries of a de novo blue copper protein by axial interactions. *JBIC, J. Biol. Inorg. Chem.* **2012**, *17* (7), 1025– 1031.

30. Plegaria, J. S.; Duca, M.; Tard, C.; Friedlander, T. J.; Deb, A.; Penner-Hahn, J. E.; Pecoraro, V. L. De Novo Design and Characterization of Copper Metallopeptides Inspired by Native Cupredoxins. *Inorg. Chem.* **2015**, *54* (19), 9470– 9482.

31. Koebke, K. J.; Ruckthong, L.; Meagher, J. L.; Mathieu, E.; Harland, J.; Deb, A.; Lehnert, N.; Policar, C.; Tard, C.; Penner-Hahn, J. E.; Stuckey, J. A.; Pecoraro, V. L. Clarifying the Copper Coordination Environment in a de Novo Designed Red Copper Protein. *Inorg. Chem.* **2018**, *57* (19), 12291– 12302.

32. Plegaria, J. S.; Pecoraro, V. L. Sculpting Metal-binding Environments in De Novo Designed Three-helix Bundles. *Isr. J. Chem.* **2015**, *55* (1), 85– 95.

33. George, G. N.; Pickering, I. J. EXAFSPAK. http://ssrl.slac.stanford.edu/~george/exafspak/exafs.htmhttp://ssrl.slac.stanford.edu/~george/exafspak/exafs.htm

34. Ankudinov, A. L.; Rehr, J. J. Relativistic calculations of spin-dependent x-ray-absorption spectra. *Phys. Rev. B: Condens. Matter Mater. Phys.* **1997**, *56* (4), R1712– R1716.

35. Weng, T.-C.; Waldo, G. S.; Penner-Hahn, J. E. A method for normalization of X-ray absorption spectra. *J. Synchrotron Radiat.* **2005**, *12* (4), 506– 510.

36. Kohzuma, T.; Shidara, S.; Suzuki, S. Direct Electrochemistry of Nitrite Reductase from *Achromobacter cycloclastes* IAM 1013. *Bull. Chem. Soc. Jpn.* **1994**, *67* (1), 138– 143.

37. Anderson, G. P.; Sanderson, D. G.; Lee, C. H.; Durell, S.; Anderson, L. B.; Gross, E. L. The effect of ethylenediamine chemical modification of plastocyanin on the rate of cytochrome f oxidation and P-700+ reduction. *Biochim. Biophys. Acta, Bioenerg.* **1987**, *894* (3), 386– 398.

38. Sharnoff, M. Electron Paramagnetic Resonance and the Primarily 3d Wavefunctions of the Tetrachlorocuprate Ion. *J. Chem. Phys.* **1965**, *42* (10), 3383– 3395.

39. Kau, L. S.; Spira-Solomon, D. J.; Penner-Hahn, J. E.; Hodgson, K. O.; Solomon, E. I. X-ray absorption edge determination of the oxidation state and coordination number of copper. Application to the type 3 site in Rhus vernicifera laccase and its reaction with oxygen. *J. Am. Chem. Soc.* **1987**, *109* (21), 6433– 6442.

40. Wijma, H. J.; MacPherson, I.; Farver, O.; Tocheva, E. I.; Pecht, I.; Verbeet, M. P.; Murphy, M. E. P.; Canters, G. W. Effect of the Methionine Ligand on the Reorganization Energy of the Type-1 Copper Site of Nitrite Reductase. *J. Am. Chem. Soc.* **2007**, *129* (3), 519– 525.

41. Solomon, E. I.; Szilagyi, R. K.; DeBeer George, S.; Basumallick, L. Electronic Structures of Metal Sites in Proteins and Models: Contributions to Function in Blue Copper Proteins. *Chem. Rev.* **2004**, *104* (2), 419– 458.

42. Ellis, P. J. *Structural Studies of Metalloproteins Using X-ray Absorption Spectroscopy and X-ray Diffraction*, PhD; University of Sydney: Sydney, Australia, 1995.

43. Hahn, J. E.; Scott, R. A.; Hodgson, K. O.; Doniach, S.; Desjardins, S. R.; Solomon, E. I. Observation of an electric quadrupole transition in the X-ray absorption spectrum of a Cu(II) complex. *Chem. Phys. Lett.* **1982**, *88* (6), 595– 598.

44. de Groot, F.; Vanko, G.; Glatzel, P. The 1s x-ray absorption pre-edge structures in transition metal oxides. *J. Phys.: Condens. Matter* **2009**, *21* (10), 104207.

45. Mann, S. I.; Heinisch, T.; Weitz, A. C.; Hendrich, M. P.; Ward, T. R.; Borovik, A. S. Modular Artificial Cupredoxins. *J. Am. Chem. Soc.* **2016**, *138* (29), 9073– 9076.

46. Den Blaauwen, T.; Van de Kamp, M.; Canters, G. W. Type I and II copper sites obtained by external addition of ligands to a His117Gly azurin mutant. *J. Am. Chem. Soc.* **1991**, *113* (13), 5050– 5052.

47. van Pouderoyen, G.; Andrew, C. R.; Loehr, T. M.; Sanders-Loehr, J.; Mazumdar, S.; Hill, H. A. O.; Canters, G. W. Spectroscopic and Mechanistic Studies of Type-1 and Type-2 Copper Sites in Pseudomonas aeruginosa Azurin As Obtained by Addition of External Ligands to Mutant His46Gly. *Biochemistry* **1996**, *35* (5), 1397– 1407.

48. Tebo, A. G.; Quaranta, A.; Herrero, C.; Pecoraro, V. L.; Aukauloo, A. Intramolecular Photogeneration of a Tyrosine Radical in a Designed Protein. *ChemPhotoChem.* **2017**, *1* (3), 89– 92.

49. Fernández, C. O.; Sannazzaro, A. I.; Vila, A. J. Alkaline Transition of Rhus vernicifera Stellacyanin, an Unusual Blue Copper Protein. *Biochemistry* **1997**, *36* (34), 10566– 10570.

50. Abdelhamid, R. F.; Obara, Y.; Kohzuma, T. Alkaline transition of pseudoazurin Met16X mutant proteins: Protein stability influenced by the substitution of Met16 in the second sphere coordination. *J. Inorg. Biochem.* **2008**, *102* (5), 1373– 1379.

51. Groeneveld, C. M.; Canters, G. W.; Aasa, R.; Reinhammar, B. EPR of azurins from pseudomonas aeruginosa and alcaligenes denitrificans demonstrates pH-dependence of the copper-site geometry in pseudomonas aeruginosa protein. *J. Inorg. Biochem.* **1987**, *31* (2), 143– 154.

52. Lancaster, K. M.; Sproules, S.; Palmer, J. H.; Richards, J. H.; Gray, H. B. Outer-Sphere Effects on Reduction Potentials of Copper Sites in Proteins: The Curious Case of High Potential Type 2 C112D/M121E Pseudomonas aeruginosa Azurin. *J. Am. Chem. Soc.* **2010**, *132* (41), 14590– 14595.

53. Den Blaauwen, T.; Hoitink, C. W. G.; Canters, G. W.; Han, J.; Loehr, T. M.; Sanders-Loehr, J. Resonance Raman spectroscopy of the azurin His117Gly mutant. Interconversion of type 1 and type 2 copper sites through exogenous ligands. *Biochemistry* **1993**, *32* (46), 12455– 12464.

54. Den Blaauwen, T.; Canters, G. W. Creation of type-1 and type-2 copper sites by addition of exogenous ligands to the Pseudomonas aeruginosa azurin His117Gly mutant. *J. Am. Chem. Soc.* **1993**, *115* (3), 1121– 1129.

55. Vidakovic, M.; Germanas, J. P. Novel Biological Copper Proteins through Anion Addition to the Mutant Met121Gly of Pseudomonas aeruginosa Azurin. *Angew. Chem., Int. Ed. Engl.* **1995**, *34* (15), 1622– 1624.

56. Bonander, N.; Karlsson, B. G.; Vänngård, T. Environment of Copper in Pseudomonas aeruginosa Azurin Probed by Binding of Exogenous Ligands to Met121X (X = Gly, Ala, Val, Leu, or Asp) Mutants. *Biochemistry* **1996**, *35* (7), 2429– 2436.

57. Samanta, S.; Lehnert, N. A switch for blue copper proteins?. *Nat. Chem.* **2016**, *8*, 639.

58. Zhang, S.; Melzer, M. M.; Sen, S. N.; Çelebi-Ölçüm, N.; Warren, T. H. A motif for reversible nitric oxide interactions in metalloenzymes. *Nat. Chem.* **2016**, *8*, 663.

59. Zhang, Y.; Cremer, P. S. Interactions between macromolecules and ions: the Hofmeister series. *Curr. Opin. Chem. Biol.* **2006**, *10* (6), 658– 663.

60. Endo, A.; Kurinomaru, T.; Shiraki, K. Hyperactivation of α-chymotrypsin by the Hofmeister effect. *J. Mol. Catal. B: Enzym.* **2016**, *133*, S432– S438.

61. Ghosh, S.; Xie, X.; Dey, A.; Sun, Y.; Scholes, C. P.; Solomon, E. I. Thermodynamic equilibrium between blue and green copper sites and the role of the protein in controlling function. *Proc. Natl. Acad. Sci. U. S. A.* **2009**, *106* (13), 4969– 4974.

62. King, J. D.; McIntosh, C. L.; Halsey, C. M.; Lada, B. M.; Niedzwiedzki, D. M.; Cooley, J. W.; Blankenship, R. E. Metalloproteins Diversified: The Auracyanins Are a Family of Cupredoxins That Stretch the Spectral and Redox Limits of Blue Copper Proteins. *Biochemistry* **2013**, *52* (46), 8267– 8275.

63. King, J. D.; Harrington, L.; Lada, B. M.; He, G.; Cooley, J. W.; Blankenship, R. E. Site-directed mutagenesis of the highly perturbed copper site of auracyanin D. *Arch. Biochem. Biophys.* **2014**, *564*, 237– 243.

64. Roger, M.; Biaso, F.; Castelle, C. J.; Bauzan, M.; Chaspoul, F.; Lojou, E.; Sciara, G.; Caffarri, S.; Giudici-Orticoni, M.-T.; Ilbert, M. Spectroscopic Characterization of a Green Copper Site in a Single-Domain Cupredoxin. *PLoS One* **2014**, *9* (6), .

65. Roger, M.; Sciara, G.; Biaso, F.; Lojou, E.; Wang, X.; Bauzan, M.; Giudici-Orticoni, M.-T.; Vila, A. J.; Ilbert, M. Impact of copper ligand mutations on a cupredoxin with a green copper center. *Biochim. Biophys. Acta, Bioenerg.* **2017**, *1858* (5), 351– 359.

66. Tegoni, M.; Yu, F.; Bersellini, M.; Penner-Hahn, J. E.; Pecoraro, V. L. Designing a functional type 2 copper center that has nitrite reductase activity within α-helical coiled coils. *Proc. Natl. Acad. Sci. U. S. A.* **2012**, *109* (52), 21234– 21239.

67. Yu, F.; Penner-Hahn, J. E.; Pecoraro, V. L. De Novo-Designed Metallopeptides with Type 2 Copper Centers: Modulation of Reduction Potentials and Nitrite Reductase Activities. *J. Am. Chem. Soc.* **2013**, *135* (48), 18096– 18107.

68. Koebke, K. J.; Yu, F.; Van Stappen, C.; Pinter, T. B. J.; Deb, A.; Penner-Hahn, J. E.; Pecoraro, V. L. Methylated Histidines Alter Tautomeric Preferences that Influence the Rates of Cu Nitrite Reductase Catalysis in Designed Peptides. *J. Am. Chem. Soc.* **2019**, *141* (19), 7765– 7775.

69. Pascher, T.; Karlsson, B. G.; Nordling, M.; Malmstrom, B. G.; Vanngard, T. Reduction potentials and their pH dependence in site-directed-mutant forms of azurin from Pseudomonas aeruginosa. *Eur. J. Biochem.* **1993**, *212* (2), 289– 296.

70. Marshall, N. M.; Garner, D. K.; Wilson, T. D.; Gao, Y.-G.; Robinson, H.; Nilges, M. J.; Lu, Y. Rationally tuning the reduction potential of a single cupredoxin beyond the natural range. *Nature* **2009**, *462*, 113.

71. Hosseinzadeh, P.; Lu, Y. Design and fine-tuning redox potentials of metalloproteins involved in electron transfer in bioenergetics. *Biochim. Biophys. Acta, Bioenerg.* **2016**, *1857* (5), 557– 581.

72. Polizzi, N. F.; Wu, Y.; Lemmin, T.; Maxwell, A. M.; Zhang, S.-Q.; Rawson, J.; Beratan, D. N.; Therien, M. J.; DeGrado, W. F. De novo design of a hyperstable non-natural protein–ligand complex with sub-Å accuracy. *Nat. Chem.* **2017**, *9* (12), 1157– 1164.

73. Boyken, S. E.; Chen, Z.; Groves, B.; Langan, R. A.; Oberdorfer, G.; Ford, A.; Gilmore, J. M.; Xu, C.; DiMaio, F.; Pereira, J. H.; Sankaran, B.; Seelig, G.; Zwart, P. H.; Baker, D. De novo design of protein homo-oligomers with modular hydrogen-bond network–mediated specificity. *Science* **2016**, *352* (6286), 680– 687.